A&A 405, 981–990 (2003)
DOI: 10.1051/0004-6361:20030651

Astronomy & Astrophysics

The RR Lyrae star period – *K*-band luminosity relation of the globular cluster M 3⋆

D. J. Butler⋆⋆

Max-Planck-Institut für Astronomie, Königstuhl 17, 69117 Heidelberg, Germany

Received 10 February 2003 / Accepted 24 April 2003

Abstract. That the RR Lyrae star period – *K*-band luminosity relation is a promising tool as a distance indicator in the Milky Way and Local Group of galaxies is apparent on observational and theoretical grounds in the literature. Less clear is the sensitivity of the relation, and consequently the physics of horizontal branch stars, to differences in stellar environment. In this paper, the first measurement of the (fundamental) period – *K*-band luminosity relation for the central region of a globular cluster is presented. It is based on a sample of seven RR Lyrae stars imaged with adaptive optics. In addition, the relation for the outer region has been reanalyzed, and is found to be in good agreement with both the previous estimate by Longmore et al. (1990), and with the inner region relation, especially when irregular and double-mode RR Lyrae stars are excluded. Importantly, there is no difference between the slope of the inner and outer region relation within measurement uncertainties, suggesting no difference in evolutionary state (luminosity). Taking the M 3 distance modulus as 15.0 ± 0.07 mag, the period–absolute *K*-band magnitude relation derived by linear least squares fitting is: $M_K = -0.96\ (\pm 0.10) - 2.42\ (\pm 0.16)\ \mathrm{Log}\, P_o$ for the inner region. Excluding irregular variable stars, the outer region relation is: $M_K = -1.07\ (\pm 0.10) - 2.38\ (\pm 0.15)\ \mathrm{Log}\, P_o$. This good agreement provides further strong support for the near-IR period-luminosity relation as a distance indicator.

Key words. stars: variables: RR Lyr – stars: distances – stars: horizontal branch – stars: imaging – instrumentation: adaptive optics

1. Introduction

For more than a century, RR Lyrae stars, in addition to classical Cepheids, have played an important role as primary distance indicators in the Milky Way and the Local Group of galaxies. The importance of RR Lyrae stars stems primarily from their brightness, being presently observable efficiently out to distances of several Mpc; they have characteristic light curves, easily measured periods, a narrow magnitude range, and a high frequency in many globular clusters, but their intrinsic luminosity is uncertain, both empirically and theoretically (see Caputo et al. 2000, and reference therein). Indeed, the dependence of intrinsic luminosity on metal content is uncertain: metal-rich and -poor RR Lyrae stars appear to follow different linear M_V – [Fe/H] relationships (Caputo et al. 2000).

In contrast, near-infrared observations of RR Lyrae stars hold several distinct advantages over optical investigations: they have a significantly weaker dependence on [Fe/H] (Bono et al. 2001); the *K*-band amplitudes of RR Lyrae variables are smaller than their *V*-band values; and their near-IR light curves are more symmetrical. All these points lead toward more easily measured and accurately determined absolute magnitudes, and importantly, with a much reduced sensitivity to reddening. The relationship between the periods and *K*-band magnitudes of RR Lyrae stars has been measured in the pioneering semi-empirical work of Longmore et al. (1990) who found a tight relationship for several galactic globular clusters. Bono et al. (2001) provided the theoretical support for these findings. They calculated the dependence of the relation on metallicity, and determined the intrinsic dispersion in the three relevant parameters, namely period, luminosity and chemical composition. Confirming the reliability of the relation further, Bono et al. (2001) applied the PL_K relation together with predicted mass and luminosity from current evolutionary models, to forecast the parallax of RR Lyr and found a good agreement with the HST result (Benedict 2002).

As quoted in the literature before, horizontal branch (HB) stars could be regarded has having crucial importance in our understanding of several unresolved astrophysical problems such as the second-parameter problem, the UV-upturn in elliptical galaxies (Ferguson 1999), as well as the dependence of the absolute *V*-band magnitude M_V of RR Lyrae stars on chemical composition.

A relevant key issue is abundance variations in stars. Abundance variations (typically of C, N, and O) have been found to occur along the whole stellar evolutionary sequence from below the turn-off of the main sequence to the red giant

⋆ Based on observations made with the NASA/ESA Hubble Space Telescope, obtained from the data archive at the Space Telescope Science Institute. STScI is operated by the Association of Universities for Research in Astronomy, Inc. under NASA contract NAS 5-26555.

⋆⋆ e-mail: butler@mpia.de

branch (RGB) in several globular clusters. It is hard to list all the significant reviews in this field, but Kraft (1994), Cannon et al. (1998), Briley et al. (2001) and references therein provide an overview of current thoughts on the subject for giant stars, while on the topic of main sequence stars, useful references can be found in Harbeck et al. (2003). RR Lyrae star luminosities, colours, and periods could be affected by inhomogeneities in the initial chemical composition of the primordial gas, internal stellar mixing processes, mass loss, and possibly multiplicity in globular clusters, and the cumulative effect of such variations may reveal themselves in precise multi-wavelength period-luminosity relation studies. It is fair to say that a database of precise, consistent measurements for a large number of RR Lyrae stars covering a range of environments (in globular clusters, the field, different galaxies, etc.) will be important for useful future tests of the intrinsic dispersion predicted by Bono et al. (2001).

In this paper, the period–*K*-band luminosity relation for the inner region ($r < 20''$) of the globular cluster M 3 is presented. As a close agreement with the outer region relation ($r > 50''$) is generally expected to exist but has not been shown, the inner and outer region relations are compared. The motivation has been to provide further support for the near-IR period-luminosity relation as a distance indicator. This work has been made possible by *K*-band adaptive optics – assisted observations.

2. Observations and data analysis

The data consists of a series of *K*-band frames taken on April 19th, 21st 2000 using natural guide star adaptive optics (AO) imaging with ALFA (Kasper et al. 2000) on the 3.5 m telescope at the German-Spanish Astronomical Centre on Calar Alto. The science camera was Omega Cass with a plate scale of $0.08''$ pixel^{-1} giving a field of view (FoV) of $80'' \times 80''$. Dithering of source frames during exposures was not performed, but there were occasional changes of guide star between exposures. Observing overheads were of the order of a few ×10%, and there were target-of-opportunity override observations at the beginning of each night. Conditions were photometric on the 19th and some light cloud was present on the 21st. The *K*-band source details are given in Table 1. On the 21st some *J*-, and *H*-band frames were taken, but are omitted as they are not within the scope of this study. The Shackhartmann wavefront sensor (WFS) FoV was set to $3''$ to block out neighbouring stars, and a signal threshold level was used to ignore faint stars in the WFS FoV. There were two suitable AO guide (or reference) stars, namely S1 ($m_V \sim 12.8$, $m_K = 9.3$) and S2 ($m_V \sim 13.2$, $m_K = 10.2$), marked in Fig. 1. A consequence of the AO correction is that the best correction occurs in the direction of the guide star, becoming worse at off-axis angles. There is no obvious evidence of systematic residuals due to radial PSF changes in the star-subtracted frames, though the central PSF flux is more pronounced toward the guide star. Through comparison with *K*-band data from Davidge & Grundahl, in preparation, which is reported in the next section, the effect on photometric measurements is up to a few percent at most, similar to reports by Davidge (2000) and references therein. The point spread function (PSF) FWHM varied between frames from about 0.3 to $0.6''$ (see Table 1) due to varying seeing, and signal-to-noise. The globular cluster M 3 (NGC 5272; $d_{\rm galactocentric} = 12.2$ kpc; Harris 1996) was selected because of its plentiful supply of RR Lyrae stars (Corwin et al., in preparation; Corwin et al. 2001; Clement 1997; Sawyer-Hogg 1973). Several potential guide stars are within the central few arc-minutes, and there is a relatively low number density of stars compared to M 15, which presently is the only other cluster with both a well studied, and plentiful *central* RR Lyrae star population (Butler et al. 1998; referred to hereafter as B98). Additionally, public Hubble Space Telescope (HST) integrations taken in 1995 April 25 are available and were retrieved from the STScI science archive. Calibration details are given by Bagget et al. (2002) and Holtzman et al. (1995). The observations consist of two 70s and two 3s Wide Field Planetary Camera 2 (WFPC2) integrations with the F336W and F555W filters respectively (referred to here as U_{336} and V_{555}). They are listed in Table 1. The U_{336} data was used to provide accurate stellar astrometry, and both filters were required for high signal-to-noise giant star magnitudes.

In the U_{336} frame, the core of M 3 is roughly centred on the Planetary Camera (PC1) chip which has the highest angular resolution ($0.045''$ pixel^{-1}). It was thus decided to concentrate on the PC1 frame only. The exact locations of stars have been obtained by reducing the Planetary Camera (PC1) frame following the procedure developed by B98. The resulting standard deviation (rms) of the astrometry residuals from a high order *U*- to *V*-band coordinate transformation are of the order of $0.0025''$ in both axes. By using this astrometry the positions of stars in the *K*-band field have been accurately located. For the present application, the simple charge transfer efficiency ramp correction of Holtzmann et al. (1995) is adequate and has been applied. The U_{336} and V_{555} have been zero point calibrated according to the Holtzman et al. (1995) recipe (their Eq. (8) and Table 7).

For the near-infrared data reduction standard IRAF[1] routines and scripts were used. The basic image frames (typically 60 s) were taken with the cluster centre positioned on one of the CCD quadrants, and a standard near-infrared reduction scheme of sky-subtraction and flat-fielding was followed. However, the measured sky frame illumination is non-uniform, varying across each camera quadrant, predominately along the readout direction. In contrast, the dome frames have a flatter appearance. The effect is such that the drop-off in illumination intensity is up to 20% in each quadrant. The cause is not clear. For correction of this effect, the parameters involved are the number of counts per pixel from the source S, the thermal signal T, and the observed signal O which is related to the normalized flat-field response (or relative quantum efficiency) of the imaging system, k, by

$$O(x, y) = k(x, y) \times S + T(x, y). \quad (1)$$

[1] IRAF is distributed by the National Astronomy Observatory, which is operated by the Associations of Universities for Research in Astronomy, Inc., under the cooperative agreement with National Science Foundation.

Table 1. Source information.

Date	UT start	Integration time s	Final[a] resolution ″	Date	UT start	Integration time s	Final[a] resolution ″	Filter
19/4/00	1 : 06 : 16	120	0.46	21/4/00	20 : 51 : 03	60	0.46	*K*
19/4/00	1 : 09 : 03	60	0.45	21/4/00	20 : 59 : 35	60	0.46	*K*
19/4/00	1 : 11 : 38	60	0.44	21/4/00	21 : 13 : 57	60	0.40	*K*
19/4/00	1 : 20 : 58	60	0.32	21/4/00	21 : 46 : 40	60	0.49	*K*
19/4/00	1 : 34 : 25	24	0.58	21/4/00	22 : 14 : 29	60	0.41	*K*
19/4/00	1 : 46 : 24	60	0.42	22/4/00	0 : 20 : 40	42	0.44	*K*
19/4/00	1 : 48 : 35	60	0.40	22/4/00	0 : 28 : 12	63	0.44	*K*
19/4/00	1 : 59 : 22	60	0.38	22/4/00	0 : 39 : 24	39	0.54	*K*
19/4/00	2 : 13 : 26	60	0.36	19/4/00	2 : 15 : 12	60	0.32	*K*
25/04/95	–	$2 \times 3/2 \times 70$	–	–	–	–	–	F555W/F316W

[a] Measured at the centre of the PC1 region, about 20″ from the guide star(s); uncertainty in spatial resolution is ~ ±0.05″.

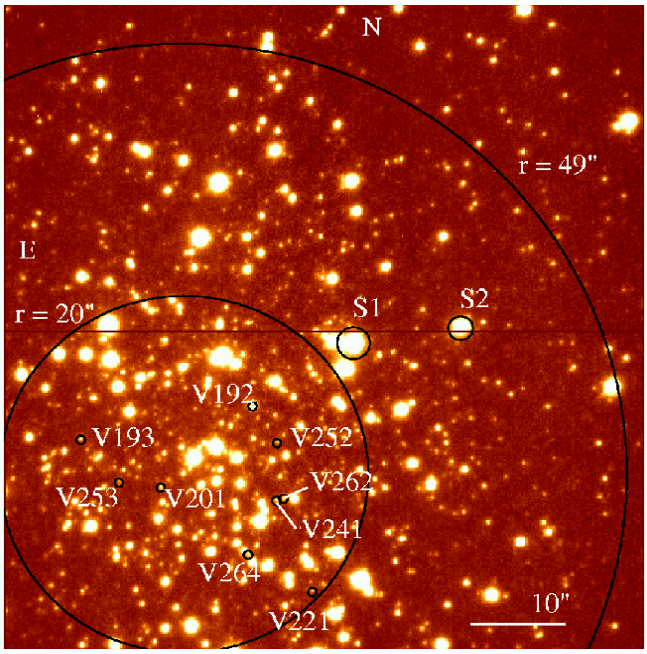

Fig. 1. Composite/cropped frame showing the central (*K*-band) field of M 3 with the two AO guide stars, S1 and S2, and relevant RR Lyrae stars marked. North (N) and East (E) directions are included.

The standard iterative procedure of fitting a low order surface function to the median filtered quadrants was applied to sky and dome flat-fields to determine the conversion image $k_{\rm sky}/k_{\rm dome}$ (where $S_{\rm dome,sky} = 1.0$). For each source image, the final flat-field was created by taking the inverse-normalized lights "on" and lights "off" dome frames in turn, then multiplying each by the appropriate conversion image, and finally taking the difference between the two of them. Importantly, this process removes the average bias and dark count in each pixel.

The next issue is sky subtraction. As *K*-band sky emission varies over time, sky frames taken close in time (less than about two minutes) to each object frame, which might otherwise swamp the light from the faintest stars, need to be subtracted. Sky frames were built by stacking image frames taken at different pointings at 300″ from the cluster centre and dithered by 10–15″. Incomplete star removal in the bottom-right chip of some median sky frames occurred due to the presence of a few close stars; but these stars are outside the PC1 region and thus have no effect on the results presented in this paper. The best fitting function $[k \times S]_{\rm sky}(S_{\rm sky} = 1.0)$ was determined for each stacked sky frame; subtraction of it from the sky frame itself yields the thermal component. As it is important to remove most of the night sky flux, the sky component (the best surface fit to the appropriate sky frames) was scaled slightly for most science frames, typically by about 1%. The thermal component, which is about 1–2% of the sky flux was then added. For hot/bad pixel removal, the flat-field was multiplied by a hot pixel mask derived from the flat-fielded sky frame. Next, for sky background removal, the flux-weighted centroid of each source frame was determined and the frames were shifted to a common centroid. This stacked source frame and the stacked sky frame, both of equal integration time, were then flat-fielded and the difference was taken.

Following the calibration of all the *K*-band frames, eleven frames with sub- half arc second spatial resolution were selected for signal-to-noise/crowding reasons, the flux-weighted centroid of each frame was determined, and all were shifted to a common centroid. This was done three times using a different set of frames at each turn to allow three high signal-to-noise estimates of the *K*-band magnitudes. In this way, a bootstrap estimate of magnitude uncertainty can be obtained later after determining the photometry. To test the internal photometric precision later using the brightest stars the individual frames were also reduced.

It is possible that analysis of the non-PC1 portion of the full *K*-band field in Fig. 1 may reveal some evidence for red giant branch variable stars that could be considered in the context of giant star evolution; but such a study is outside the scope of this paper.

2.1. Photometry

The photometric reductions have been carried out using the DAOPHOT (Stetson 1987) photometry package. The procedure used to derive U_{336} and V_{555} instrumental magnitudes, is taken from that described by B98. The V_{555} astrometry is estimated to be complete down to

$V_{555} = 17$ ($K < 15$ for $(V-K)_{\rm giants} < 2$) based on insertion of artificial stars into the V_{555} frame and repeating the data reduction.

PSF-fitting was performed using the routine ALLSTAR (Stetson & Harris 1988), part of the DAOPHOT package. Each K-band frame has been considered as two sections overlapping by 20″, and the following procedure for each section, taken partly from B98, has been carried out: the initial PSF was obtained using standard recursive techniques; the star list at this point consisted only of stars detected by DAOFIND, which typically found about 250–300 in the PC1 region. This allowed a high-order coordinate transformation between the K-band frames and the HST/PC1 field, thereby accounting for relative geometrical distortion near known RR Lyrae stars in the field. 60–90 stars were selected from each section. After applying this transformation, one for each section, to the HST/PC1 star list, the rms positional accuracy was of the order of 0.02″ in both axes. Then, a background-subtracted image and its PSF were fed into the PLUCY (Hook et al. 1994) restoration task in IRAF. Although not photometrically reliable, the data from the restoration task provided good initial magnitude estimates for the brightest stars in the field. Together with these magnitudes, accurate coordinates, sky background estimates and a unique ID number for each star, a final PSF fitting could be performed. Next, U_{336}[2] background estimates were scaled up appropriately, followed by re-making the PSF, and transformation of the list fitted by ALLSTAR using the new star IDs, in groups of 500 stars; the sky background is re-calculated for each star individually rather taking a group estimate as the background varies significantly across the field. Finally, the photometry from each section was tied to the same internal zero point. This step was performed by taking a calibration of a sequence of stars in the range $K < 17$ against their counterparts in an average dataset. Firstly, the histogram of individual offsets, typically forming a normal-like distribution, was created. Then, in an iterative process, histogram outliers were ignored until two different estimates of the zero point offset, the weighted-histogram average and median value, differed by less than 0.01 mag. In this way, the calibration of the K-band magnitude zero point is on a robust statistical footing, insensitive to large amplitude variable stars and photometry outliers.

In the context of photometric precision, it is worth mentioning that a space-invariant empirical PSF made using 2–4 of the brightest stars, and modeled on a moffat elliptical function of index 1.5 works best because the background light due to the faint unresolved stellar population is distributed in an inhomogeneous way. As there is a pointing difference of about 12″ for some frames, it was possible to test the photometric precision along both axes for each individual frame; for this, the way in which magnitudes differ from their time averaged/intensity weighted average was examined. No obvious indication of a trend with field position was found.

[2] The light from the undetected stellar population is dominated by light from upper main sequence stars in a narrow colour range; the deviation from the mean colour for the bulk of these stars over the field is expected to be up to a few tenths of a magnitude.

For validation of the quality of the instrumental magnitudes a sequence of stars in the range $K < 17$ was calibrated against their counterparts in Canadian-France-Hawaii Telescope AO data from Davidge & Grundahl (2002, in preparation; referred to here as DG). Davidge & Courteau (1999) reported an absolute zero point error of ±0.009 mag for their K-band magnitudes which came from CFHT AO observations; but conservatively, $\sigma_K = 0.05$ mag is assumed for the DG data. The difference between the intensity weighted average $K_{\rm PC1}$ and the DG data are compared in Fig. 2; and known RR Lyrae stars from Corwin et al. (2002, in preparation) are marked with open circles. Apart from the outlying RR Lyrae star which may be a false measurement due to stellar crowding, there is a good agreement. In Fig. 3 the rms scatter is plotted as a function of K for stars in the PC1 region with at least two (out of three) data points (bottom); and (top) for stars in common with the $K_{\rm DG}$ data for which at least two $K_{\rm PC1}$ data points have been measured. It can be seen that the rms value in the RR Lyrae star magnitude range is about 0.05 mag, caused by both intrinsic variability and photometric error. It is useful to note that intrinsic K-band amplitudes of RR Lyrae stars of type RRab are up to a few tenths of a magnitude, and smaller for RRc-type variables.

For zero point validation, the Cohen et al. (1978; referred to hereafter as C78) giant branch data was considered. The $V-K$ colour of their M 3 giant branch ridgeline at $M_K = -3.0$ ($\sigma_{V-K} = \pm 0.03$ mag) was checked and compared with the value found on the Ferraro et al. (2002; referred to hereafter as F00) ridgeline for globular clusters with a similar metallicity to M 3; [Fe/H] = −1.34 dex from Carretta & Gratton (1997) is adopted. A good agreement was found to within ±0.05 mag. Next, in order to convert the F00 ridgeline M_K to K-band magnitudes, a distance modulus of 15.00 ± 0.07 mag (Caputo et al. 2000) (see Sect. 3.1 later for a discussion) was assumed and the V/K data was overlaid with the C78 V/K giant star data on the (V, $V-K$) colour magnitude diagram in Fig. 4. A solid line fit to the C78 data (excluding the outliers (asterisks)) is included. The slight mismatch in ridgelines close to the tip of the RGB arises because the corresponding metallicity of the F00 line is only similar but not equal to that of M 3. The lower end of the RGB is much less metal-sensitive, and so, as confirmed above, it is safe to compare the ridgelines at two or more magnitudes fainter than the RGB Tip. Taking the C78 data as the reference dataset, the offset between the C78 and F00 lines suggests that the lower end of the C78 ridgeline comprises asymptotic giant branch (AGB) stars at $V > 13.5$. Next, the (V_{555}, $V_{555} - K_{\rm PC1}$) colour magnitude diagram for stars with $\sigma_K < 0.03$ mag and $\sigma_{V,555} < 0.05$ mag (the V-band zero point error is ±0.05 mag) was overlaid with the $K_{\rm PC1}$ magnitudes shifted by -0.1 ± 0.05 mag to match the lower end of the RGB fiducial ridgeline for [Fe/H] = −1.34 dex, (dot-dashed/thick) which was deduced from the F00 (V-K)–[Fe/H] relations.

2.2. Deriving $< K >$

The epochs of individual K-band frames are distributed over 20–50% of RR Lyrae star light curve cycles. Uncorrected,

the measured average magnitude for each variable might differ from the intrinsic average value which is required for the PL_K relation. This fact is also true for the deep/composite frames that are considered here for signal-to-noise reasons. The adopted way to tackle this issue is taken from Jones et al. (1996; referred to hereafter as J96): based on template near-IR light curves for both RRab- and RRc-type variables, the method allows the offset from the true mean magnitude to be estimated if the period, optical amplitude, and light curve phase of each exposure is known. By taking frames from different light curve phases, template shifting acts to minimize deviations from the true mean magnitude arising from uncertainties in emphemeris phase (J96). For this reason, the magnitude offset associated with each composite frame is determined by calculating the offset associated with each of its constituent frames, and then summing these values, weighted by the constituent integration times. The magnitude offset associated with each star in any of the deep frames is in the range −0.05 to 0.03 mag. The error reported for the J96 recipe is typically less than 0.03 mag; however, for each deep frame there are eleven frames covering a range of light curve phases, leading to a negligible average error, and is ignored.

Zero-pointed photometry for a sample of seven RR Lyrae stars, labelled in Fig. 1 according to Bakos et al. (2000), was matched to their associated periods (see Table 2). The RR Lyrae stars comprise five stars of the type RRab and two stars of the type RRc. Period data with a precision better than 1% is taken from CC01, Corwin (2002, in preparation) and Strader et al. (2002). The epochs in Table 2 are taken from CC02 which is based on their earlier work (CC01). The CC01 study made use of observations made on six nights in 1992, seven nights in 1993 and one night in 1997. The observations for the present study were made in 2000. Of the inner region variables considered in this paper all have a precise emphemeris, (except V253 for which none has been reported). It turns out that the results in this paper are insensitive to a random choice of emphemeris for this star, as might be expected for an intrinsically low amplitude variable. No period change has been measured by CC01 for the inner region sample considered here, although period change rates up to about 0.5 days Myr^{-1} were found for 38 outer region RR Lyrae stars. Even if such changes were common to each star, it is reasonable to believe that the ephemerides that CC01 published are valid for 2000. Incidentally, the robustness of the PL_K technique to period uncertainties is further strengthened by the template shifting mentioned earlier which causes considerable reduction in errors arising from errors in the light curve phases. *B*-band amplitudes with a precision better than 5% are available from CC01 for two of the variables ($A(B)_{V193}$ = 1.6; $A(B)_{V201}$ = 1.6) and has been estimated for the remaining five variable stars using the $A(B)$–period plot of CC01. As noted later in Sect. 3, adopting a conservative error of ±0.3 mag for any of the *B*-band amplitudes, produces a change in the measured slope of the period–luminosity relation of up to ±0.01 mag and an even smaller error in the zero point of the relation.

Another issue is the possible presence of Blazko variables in the inner region sample of RR Lyrae stars – the light curve shapes of such Blazko-type stars could change on timescales of weeks or months. As none of the stars are labelled as Blazhko-type variables in CC01 or CC02, there is no "a priori" reason to suspect the presence of such variables in the available sample but the possibility remains. However, inspection of CC01's *B*-band light curves for Blazhko variables indicates that typical amplitude changes are up to about 0.5 mag, in which case the derived PL_K would be relatively insensitive to the effect.

Next, the intensity weighted average of the magnitudes determined from the three deep frames is considered. For stars with at least two valid measurements, the adopted recipe for intensity weighted averaging of photometry is this: the magnitudes for each star are converted into a flux level with a certain zero point, averaged and converted back to magnitudes. The rms value was calculated for each star; they vary in the range 0.02–0.05 mag. For line fitting later, the instrumental magnitude error for each RR Lyrae star is taken as the average (arithmetic mean) of the rms values for the seven variable stars, scaled down by $\sqrt{3}$, leading to 0.03 mag. In this way, statistical differences in magnitude errors are smoothed out. The rms value is included in the measurement of the slope of a linear fit to the period versus *K*-band relation described in the next section.

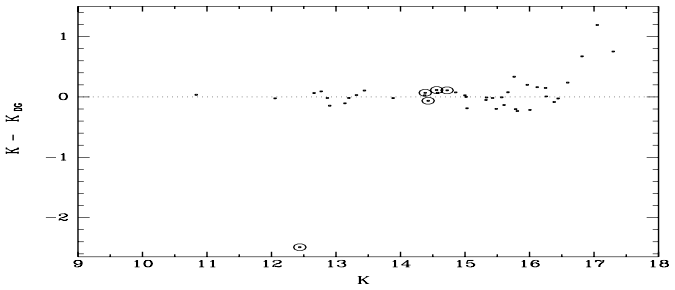

Fig. 2. Difference between the intensity weighted ensemble average *K*-band photometry from this work and DG as a function of *K*-band magnitude. The RR Lyrae stars in common between the two data sets are marked with open circles. The circled outlier may be a false measurement due to stellar crowding.

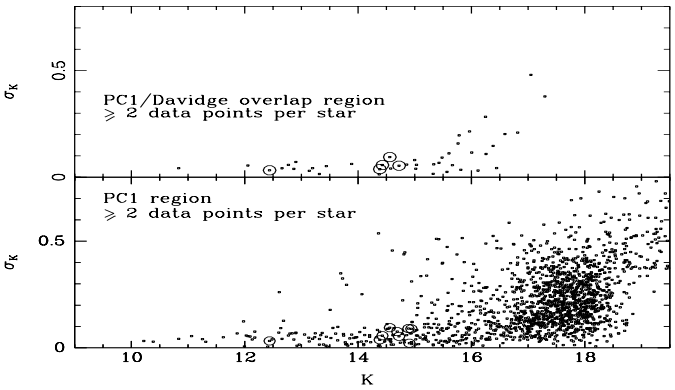

Fig. 3. σ_K is plotted as a function of mean K_{PC1} magnitude. *Top:* stars in common with the DG *K*-band data with at least two data points. The five known RR Lyrae stars in common are marked with open circles in both plots at $K \sim 15$; the circled point at about $K = 12.4$ is an outlier in Fig. 2 and may be a false measurement due to stellar crowding. *Bottom*: stars in the PC1 region with at least two data points. Nine known variable stars (tabulated in Table 2) are marked with open circles.

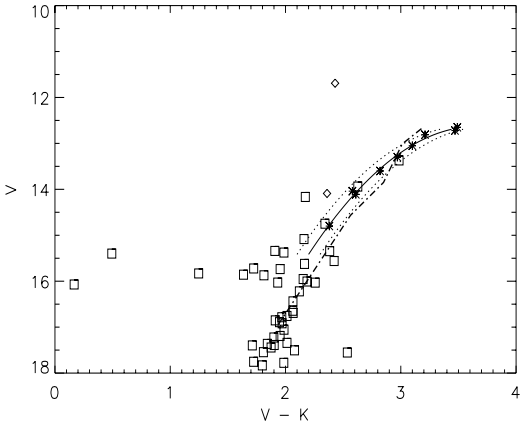

Fig. 4. *K*-band zero point offset assessment. (V_{555}, $V_{555} - K_{\rm PC1}$) CMD (squares) where $K_{\rm PC1}$ magnitudes have been shifted to match the lower end of the RGB fiducial ridgeline (dot-dashed/thick) deduced from the work of Ferraro et al. (2002; referred to hereafter as F00) taking a distance modulus of 15.0. The Cohen et al. (1978; referred to hereafter as C78) giant branch data (asterisks and diamonds) has been considered for the purpose of zero point validation; taking the C78 data as comprising asymptotic giant branch (AGB) stars at $V > 13.5$, the 2nd order polynomial/least squares fit to the C78 data (excluding the outliers (diamonds) falls within ±0.05 mag of the apparent AGB stars in the $K_{\rm PC1}$ data. A ±0.1 *K*-band magnitude envelope (dotted) has been included for convenience. See the final paragraph of Sect. 2.1 for more information.

The error in the absolute zero point of the *K*-band photometry from three deep frames is $\pm\sqrt{3} \times 0.01$ mag (relative zero pointing error); plus the error in the zero point offset is ±0.05 mag (systematic), leading to an absolute zero point error of ±0.053 mag.

2.3. Results

2.3.1. Inner region

The fundamental period $P_{\rm o}$ has been calculated for first-overtone (RRc) periods using the conversion $\mathrm{Log}\, P_{\rm o} = \mathrm{Log}\,(P_{\rm RRc}) + 0.127$ (Iben 1974), and is plotted against the calculated mean *K*-band magnitude for each star in Fig. 5 (top-left). Of the nine RR Lyrae stars with *K*-band magnitudes two stars V192, and V262 are outside the $\pm 1\sigma$ envelope in Fig. 2 as they are systematically too bright; only V262 is plotted in Fig. 5 for the sake of presentation but the measured mean magnitude and uncertainty are given for both in Table 2. V192 is displaced to a brighter magnitude than the longest period RR Lyrae star; CC01 classified the star as an RRab-type variable with $P = 0.481$d, $B = 14.94$, $(B - V) = 0.554$, and noted it as a blend in their data. For comparison, RR Lyrae stars observed in M 3 by CC01 have *B*-band magnitudes as bright as ∼15.8. As V192 is an outlier it is ignored in subsequent discussions. The second outlier is V262 which is marked with an open square in the left panel and has a small standard error (0.02 mag). For the seven remaining RR Lyrae stars there are three mean magnitude estimates, and the intensity weighted average is taken; one exception is V221 for which one measurement appears to be spuriously faint by 0.3 mag and the remaining two are used to estimate the average. For the measurement of the slope of the PL_K relation, σ_K, is taken to be ±0.03 mag (rms internal scatter). Both the data and the line fit are shown in Fig. 5 (left-top). Coefficients of the relation are tabulated in Table 3. The error in the true zero point of the relation is made up of the error in the absolute zero point (±0.053 mag) of the *K*-band photometry plus (in quadrature) the error in the PL_K zero point calculated by the line fitting (±0.05 mag) which leads to ±0.073 mag. An additional error must be included for the M_K–period relation. For reasons explained in Sect. 3.1, the adopted distance modulus is 15.07 ± 0.07 mag, which leads to a zero-point error of $\sigma_{M_K,\,\mathrm{zero\,pt.}} = \pm 0.10$ mag in the relation. For different future distance modulii this uncertainty must be changed accordingly.

Out of academic interest, the relation for the photometrically superior DG data set ($FWHM \sim 0.14''$) is plotted in Fig. 5 (top-right), shifted by −0.1 mag ± 0.05 mag to match the $K_{\rm PC1}$ -band photometry (zero pointed to C78); conservatively, the uncertainty in the DG photometry is taken to be 0.05 mag for the line fitting. The outlier marked with an open square at $K = 15.87$ is V215 in CC01 and has been ignored during line fitting. There is a significant difference between the best fit line in this panel and that of the outer region relation (bottom), most likely because no J96 correction has been applied as the observing epoch is absent.

2.3.2. Outer region

The work by Corwin & Carney (2001; referred to here as CC01) provides up to date information on RR Lyrae star periods and classification for the outer cluster region. The Longmore et al. (1990; hereafter referred to as L90) data was reanalyzed using the new periods for the cases of inclusion and exclusion of stars classified as Blazhko or double-mode (RRd) RR Lyrae stars. In this way, the sensitivity of the slope to these stars can be estimated, in addition to improving the precision of the relation. *K*-band magnitudes were taken from L90 which have an error $\sigma_K = \pm 0.06$ mag, and the latest period values come from CC01. There are 48 stars with *K*-band magnitudes from the L90 study, and they cover the radial range 2.6–13.3 arcmin. Of these stars, 37 are now known to be of type RRab, nine are of type RRc, one is of type RRd and one, V113, is not in the CC01 catalogue of variable stars in M 3. However, V113 has been recorded by Szeidl (1965) as an RR Lyrae star and is therefore included. The period of V113 used by L90 is 0.513d; the same value is recorded in the Clement (1997) catalogue of variable stars. V113 is not classified by Clement (1997) but is fairly safe to take it as an RRab-type variable based on its period. The RRd star, and 15 of the RRab stars which are classified as Blazhko (irregular) RR Lyrae stars by CC01 have been ignored for the fitting; they are marked by open circles in Fig. 5 (bottom). The gradient and zero point of the PL_K relation are tabulated in Table 3 for the cases of inclusion and exclusion of irregular RR Lyrae stars (rows 2 and 3 respectively). The error in the zero point of the absolute PL_K relation consists of ±0.06 mag (internal zero point error); ±0.04 mag (rms fitting error); and ±0.07 mag (distance

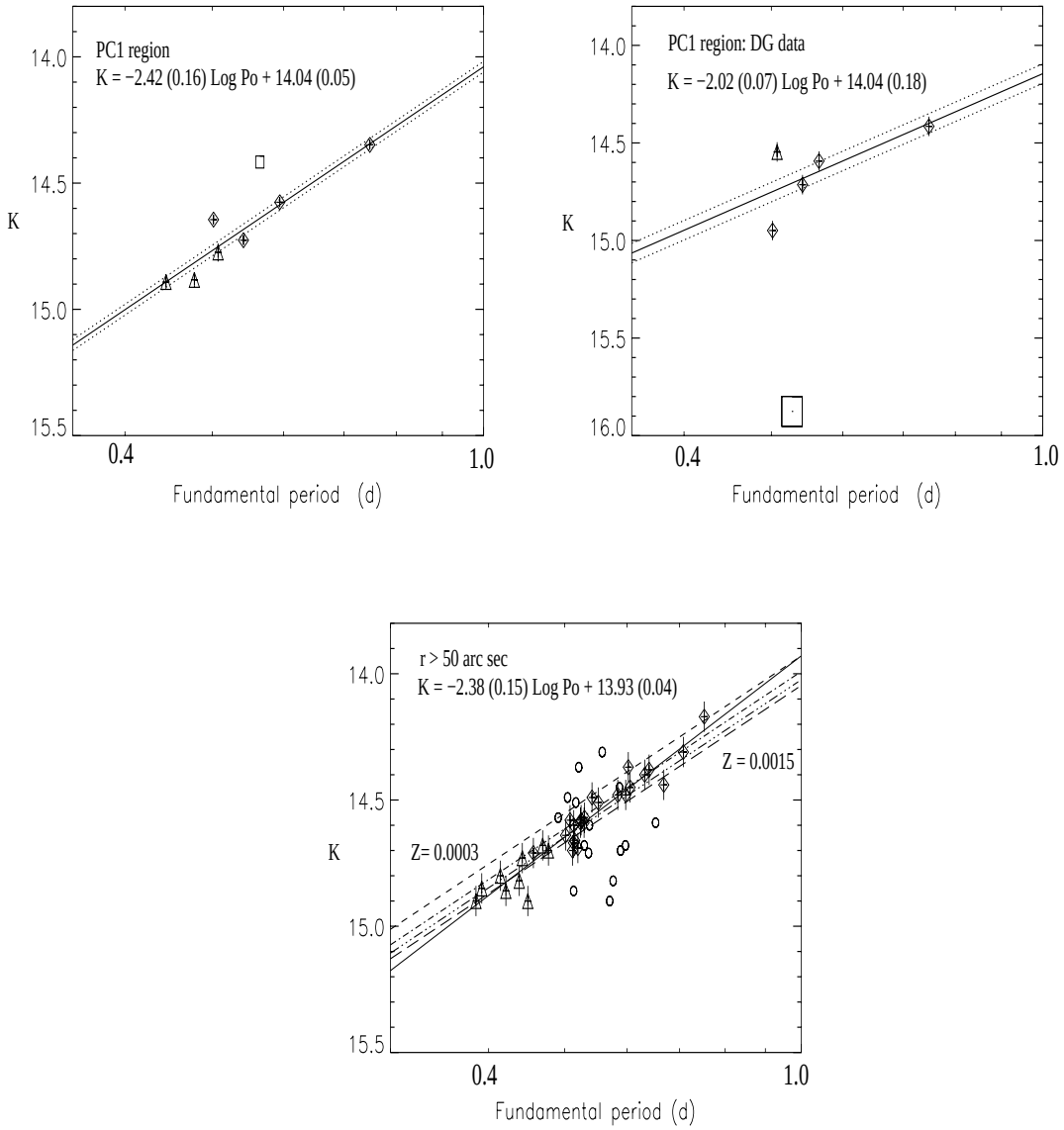

Fig. 5. Linear least squares fit to the K-band magnitude / period data (solid). The dotted lines form the 1σ envelope of the linear least squares fit to the data. Coefficient errors of the general relation $a \log P_o + b$, arising from the line fitting are given in parentheses. *Top-left:* diamonds and triangles mark the RRab- and RRc-type RR Lyrae stars respectively. *Top-right:* DG data shifted by –0.1 mag to match the K_{PC1} data (zero pointed to match C78), with no J96 offset applied as the epoch is unavailable. The open square marks an outlying star; it is V215 (K = 15.87 mag in the DG data and is not in the K_{PC1} data). *Bottom:* outer region data. Z = 0.0003, 0.0007, 0.0011 and 0.0015 tracks are overlaid (from upper to lower tracks). Data points marked with open circles are the Blazhko (irregular) stars and one RRd-type RR Lyrae star. See text in Sect. 2.3 for further information.

modulus uncertainty – referred to in the previous section). This leads to a zero point error of ±0.10 mag.

3. Discussion

3.1. Harmony in the PL_K relation

Together with accurate period data from the literature, the K-band observations prove on good photometric grounds that there is no apparent difference between the inner and outer region PL_K relation. This conclusion is based on the following:

1. The gradient of the inner region relation is weakly dependent on the way $< K >$ is calculated (intensity- or magnitude-weighted average) as shown in Table 3. The agreement is dependent on the J96 magnitude correction for RRab-type stars; excluding the correction produces a significantly steeper slope. The agreement between the inner and outer region relation is not dependent on uncertainty in $A(B)$; an error of ±30% in any of the amplitudes produces a change in slope of ±0.01, which is negligible compared to fitting errors, and an even smaller error in the zero point. For both the inner and outer region relations, periods from CC01/CC02 (and Clement 1997 in the case of V113) are well determined to a precision significantly better than 1%. CC01 mean B-band magnitudes are precise to at least 5%.

2. The absolute K-band extinction, A_K, can be derived using $A_K/E(B-V) = 0.13$ (Cardelli et al. 1989). As $E(B-V) = 0.01$ (Dutra & Bica 2000) which is negligible, no correction has

been made for K-band atmospheric extinction which would be of the order of 0.001 mag.

From these findings I conclude the following:

1. Including the irregular variables, but taking improved periods, there is good agreement between the L90 slope measurement -2.35 ± 0.15 for the outer region and value from an updated analysis of the L90 data (-2.35 ± 0.14). There is also a fine agreement with the ensemble average of the relation -2.338 ± 0.067 determined by Frolov & Samus (1998) who reanalyzed the period/K-band magnitude data tabulated by L90 for nine galactic globular clusters.
2. Inclusion or exclusion of the irregular variable stars has marginal impact on the gradient and zero point of the relation (see Table 3, rows 2 and 3); this arises because the irregular stars are well-distributed about the PL_K line.
3. There is good agreement between the PL_K relation for the inner and outer regions (see Table 3, rows 1, 2, and 3).
4. For the absolute K-band magnitude–period relation, the distance modulus to taken to be 15.0 ± 0.07 mag (Caputo et al. 2000, hereafter referred to as C00) and the reasoning behind the value chosen is explained as follows: It is true that the distance modulus for M 3 is uncertain with values in the range 14.8–15.2 appearing in the literature (C00). Setting observational errors aside for the sake of clarity, the uncertainty arises because in order to measure a distance modulus in a certain bandpass, the average magnitude of a sample of RR Lyrae stars in that bandpass, corrected for reddening, is measured through observations while the absolute magnitude is estimated through modeling. Thus, as a metallicity and a luminosity must be assumed for modeling, affecting the model stars' magnitude differently in different bandpasses, there may be a mismatch between the distance modulus derived for one bandpass and the value derived for another bandpass. However, Bono et al. (2001) report a way to find an average luminosity for RR Lyrae stars by determining the luminosity that gives the same visual and IR distance modulus, thereby yielding a mean distance modulus. For M 3 they find $(m - M)_K = 15.03 \pm 0.07$ mag which they note as being in good agreement with the mean V-band distance modulus of 15.00 ± 0.07 mag derived by C00. As Bono et al. (2001) concluded for this point, this harmony proves the internal consistency of the pulsation modeling and reinforces the belief in the literature that the reddening towards M 3 is almost zero. Adopting the C00 distance modulus for the inner region relation, the absolute K-band magnitude for the inner region is:

$$M_K = -0.96 \pm 0.10 - 2.42 \pm 0.16 \,\mathrm{Log}\, P_\mathrm{o}. \quad (2)$$

There is good agreement with the slope of the empirical metal-free relation available in the literature provided by Jones et al. (1992),

$$M_K = -0.88 \pm 0.06 - 2.33 \pm 0.20 \,\mathrm{Log}\, P_\mathrm{o} \quad (3)$$

which differs significantly from the slope of

$$M_K = -1.07 \pm 0.10 - 2.95 \pm 0.10 \,\mathrm{Log}\, P_\mathrm{o} \quad (4)$$

by Skillen et al. (1993). For the outer region, excluding irregular variables, one has

$$M_K = -1.07 \pm 0.10 - 2.38 \pm 0.15 \,\mathrm{Log}\, P_\mathrm{o}. \quad (5)$$

3.2. Comparison with theory

Bono et al. (2001) have recently calculated the theoretical PL_K relation using non-linear convective stellar pulsation models over the range of stellar temperatures covered by the instability region. They considered a range of masses, chemical composition, and luminosities, and then assessed the sensitivity of the relation to these parameters. They derived that absolute K-band magnitude of RR Lyrae stars with metal content in the range $0.0001 < Z < 0.006$ is correlated with period and metallicity as

$$M_K = 0.139 - 2.07(\mathrm{Log}\, P_\mathrm{o} + 0.30) + 0.167 \,\mathrm{Log}\, Z \quad (6)$$

with a total intrinsic dispersion of $\sigma_K = 0.037$ mag, including a luminosity uncertainty of $\Delta \mathrm{Log} L \sim \pm 0.04$, and mass variations of 4%.

The empirical study of L90 found good agreement between the PL_K relations measured for several galactic globular clusters which suggests that both the evolutionary (i.e. luminosity) effects and the spread of stellar masses inside the instability strip marginally affect that relation. On the theoretical side, Bono et al. (2001) concluded that for a certain metallicity the predicted PL_K relation is marginally dependent on stellar mass uncertainties. A mass difference would appear as a zero point offset in the PL_K relation. In this context, it is worth remarking that CC01 tentatively suggested a possible scenario to explain the presence of some optically sub-luminous RR Lyrae stars observed toward the central region of M 3, namely that collisions due to stellar crowding might prematurely halt core helium burning, leading to a lower luminosity than normal.

Another relevant issue is metallicity. Reviewing the literature, one has

$$M_K = -0.647 - 1.72 \,\mathrm{Log}\, P_\mathrm{o} + 0.04\,[\mathrm{Fe/H}] \quad (7)$$

$$M_K = -0.76 - 2.257 \,\mathrm{Log}\, P_\mathrm{o} + 0.08\,[\mathrm{Fe/H}] \quad (8)$$

and

$$M_K = -0.72 \pm 0.11 - 2.03 \pm 0.11 \mathrm{Log}\, P_\mathrm{o} + 0.06 \pm 0.08\,[\mathrm{Fe/H}] \quad (9)$$

by L90, Liu & Janes (1990), and Jones et al. (1992) respectively. Setting $[\mathrm{Fe/H}] = -1.34$ dex (Carretta & Gratton 1997) in Eqs. (7) and (8) gives $M_K = -0.18$ and -0.19 mag respectively for $\mathrm{Log}\, P_\mathrm{o} = -0.3$. Equation (9) gives a similar result. In contrast, the IR flux method that gives Eq. (5) yields $M_K = -0.36$, which is significanty brighter; this is the same discrepancy noted by L90 and Bono et al. (2001). Next, adopting a distance modulus of 15.0 mag, tracks of constant Z were derived from Eq. (6) and overlaid in Fig. 5 (bottom). Measurement errors, especially in the zero point forbid a useful fit, but there is fair qualitative agreement between the data and $\log Z = -3.04$ dex which corresponds to the adopted M 3 metal abundance $[\mathrm{Fe/H}] = -1.34$ dex. It is hard to draw a more substantial conclusion from the graph due to L90 measurement uncertainties (± 0.06 mag) and the distance modulus uncertainty (± 0.07 mag). Solving Eq. (6) yields $M_K = -0.367$ mag in fine agreement with the IR flux method (Eq. (5)). Hence, the PL_K

Table 2. Relevant details for nine variable stars from CC02 in the K_{PC1} field.

ID	Epoch (JD)	Period (days)	Type	$< K >$ (mag)	$A(K)$ (mag)	$A(B)$ (mag)
(1)	(2)	(3)	(4)	(5)	(6)	(7)
v192	2449090.225	0.49790	?	12.44[b]	-	-
v193	2449090.327	0.74784	RRab	14.35	0.34 ± 0.01	1.6[d] ± 0.1
v201	2449090.133	0.59408	RRab	14.73	0.34 ± 0.01	1.6[d] ± 0.1
v221	2449090.125	0.378752	RRc	14.77	0.27 ± 0.03	0.75 ± 0.3
v241	2449090.014	0.59408	RRab	14.58	0.28 ± 0.03	1.0 ± 0.3
v252	2449090.157	0.50155	RRab	14.64	0.33 ± 0.03	1.5 ± 0.3
v253	-	0.33161	RRc	14.89	0.27 ± 0.03	0.75 ± 0.3
v262	-	0.5647[a]	-	14.41[c]	0.29 ± 0.03	1.1 ± 0.3
v264	2448755.093	0.35649	RRc	14.88	0.27 ± 0.03	0.75 ± 0.3

Inner region variable stars.
Column (1) ID. V241 and V252 are X17 and KG4 respectively in CC01/CC02; (2) Julian date from CC02; (3) Periods. All from CC02 except [a] Strader et al. (2002); (4) RR Lyrae type from CC02; (5) Intensity-weighted K-band magnitude, $\sigma_K = \pm 0.03$ mag (random), plus ±0.05 (systematic) or ±0.058 mag combined; [b] ignored as it is an outlier. No J96 correction applied as the magnitude is inconsistent with an RR Lyrae star; [c] is an ignored outlier in Fig. 5 (top-left). (6) Expected K-band amplitudes determined by applying Eq. (7) of J96.; (7) [d] from CC01. A conservative error has been adopted. Other $A(B)$ values were taken with conservative errors from the CC01 $A(B)$ - period graph, their Fig. 9.

Table 3. Coefficients of the general relation $< K >= a \,\mathrm{Log} P_o + b$. Values in parentheses are the uncertainties; "int" and "mag" indicate where intensity- and magnitude-weighted average magnitudes respectively have been used.

Region	$\mathrm{Gradient}_{\mathrm{int}}$	$\mathrm{Zero\ point}_{\mathrm{int}}$	$\mathrm{Gradient}_{\mathrm{mag}}$	$\mathrm{Zero\ point}_{\mathrm{mag}}$	Comment
	a	b	a	b	
Inner	–2.42 (0.16)	14.04 (0.05)	–2.40 (0.17)	14.04 (0.05)	this study
Outer	-	-	–2.38 (0.15)	13.93 (0.04)	new analysis of L90 data, excluding Blazhko variables
Outer	-	-	–2.35 (0.14)	13.95 (0.04)	new analysis of L90 data, including Blazhko variables
Outer	-	-	–2.35 (0.15)	13.95 (0.04)	L90 included Blazhko variables

relation, a metal-free relation, is in good agreement with the predicted PLZ_K relation, meaning that the observations are fairly well matched by the results of stellar evolutionary models. This study cannot address the issue of intrinsic dispersion in the PL_K relation for signal-to-noise reasons. Incidentally, the signal-to-noise ratio of stars in the central regions of globular clusters is affected by stellar crowding quite severely. To explore the physics of stellar evolution and pulsation theory through the PL_K relation in the central regions of globular clusters, very high angular resolution imaging is required, and is becoming available with adaptive optics assisted near-IR imagers, such as NAOS-CONICA on the ESO VLT, and later with NIRCam on the James Webb Space Telescope.

Acknowledgements. The support of S. Hippler, M. Kasper, and the rest of the ALFA-team during observations is much appreciated. T. Davidge is thanked for providing his K-band magnitude data, as is M. Corwin for the updated list of RR Lyrae stars with their periods. The author acknowledges the support of the research and training network on "Adaptive Optics for Extremely Large Telescopes" under contract HPRN-CT-2000-00147. It is a pleasure to thank the anonymous referee for several very helpful comments and suggestions.

References

Baggett, S., McMaster, M., Biretta, J., et al. 2002, in HST WFPC2 Data Handbook, v. 4.0, ed. B. Mobasher, Baltimore, STScI
Benedict, G. F., McArthur, B. E., Fredrick, L. W., et al. 2001, ApJ, 560, 907
Bakos, G. A., Benko, J. M., & Jurcsik, J. 2001, 2000, AcA, 50, 221
Bono, G., Caputo, F., Castellani, V., & Marconi, M. 2001, MNRAS, 326, 1183
Briley, M. B., Smith, G. H., & Claver, C. F. 2001, AJ, 122, 2561
Butler, R. F., Shearer, A., Redfern, R. M., et al. 1998, MNRAS, 296, 379
Cannon, R. D., Croke, B. F. W., Bell, R. A., Hesser, J. E., & Stathakis, R. A. 1998, MNRAS, 298, 601
Caputo, F., Castellani, V., Marconi, M., & Ripepi, V. 2000, MNRAS, 316, 819
Cardelli, J. A., Clayton, G. C., & Mathias, J. S. 1989, ApJ, 345, 245
Carretta, E., & Gratton, R. G. 1997, A&AS, 121, 95
Clement, C. 1997, VizieR On-line Data Catalog: V/97, Updated 3rd Catalogue of Variable Stars in Globular Clusters
Cohen, J. G., Persson, S. E., & Frogel, J. A. 1978, ApJ, 221, 788
Corwin, M. T., & Carney, B. W. 2001, AJ, 122, 3183
Davidge, T. 2000, AJ, 119, 748
Davies, R., Eckart, A., Hackenberg, W., et al. 2000, Expt. Ast., 10, 103
Dutra, C. M., & Bica, E. 2000, A&A, 359, 347
Ferarro, F., Montegriffo, P., Origlia, L., & Fusi Pecci, F. 1999, AJ, 119, 1282

Ferguson, H. C. 1999, Ap&SS, 267, 263
Frolov, M. S., & Samus, N. N. 1998, PAZh, 24, 209
Harris, W. E. 1996, AJ, 112, 1487
Harbeck, D., Smith, G. H., & Grebel E. K. 2003, AJ, 125, 197
Holtzman, J., Burrows, C. J., Casertano, S., et al. 1995, PASP, 107, 1065
Hook, R. N., Lucy, L. B., Stockton, A., & Ridgway, S. 1994, ST-ECF Newsletter 21, 16
Iben, I. Jr. 1974, ARA&A, 12, 215
Jones, R. V., Carney, B. W., Storm, J., & Latham, D. W. 1992, ApJ, 386, 646
Jones, R. V., Carney, B. W., & Fulbright, J. P. 1996, PASP, 108, 877
Kasper, M., Looze, D., Hippler, S., et al. 2000, Exp. Ast., 10, 49
Kraft, R. P. 1994, PASP, 106, 553
Liu, T., & Janes, K. A. 1990, ApJ, 354, 273
Longmore, A. J., Dixon, R., Skillen, I., Jameson, R. F., & Fernley, J. A. 1990, MNRAS, 247, 684
Sawyer-Hogg, H. 1973, Publ. of The David Dunlop Observatory of Toronto, 3, 6
Skillen, I., Fernley, J. A., Stobie, R. S., & Jameson, R. F. 1993, MNRAS, 265, 301
Strader, J., Everitt, H. O., & Danford, S. 2002, MNRAS, 335, 621
Szeidl, B. 1965, Commun. Konkoly Obs., 58, 1